DEUTSCHES ELEKTRONEN – SYNCHROTRON

DESY 93-047
April 1993

Results from Pion Calibration Runs for the H1 Liquid Argon Calorimeter and Comparisons with Simulations

H1 Calorimeter Group

ISSN 0418-9833

NOTKESTRASSE 85 · D-2000 HAMBURG 52

To be sure that your preprints are promptly included in the HIGH ENERGY PHYSICS INDEX, send them to (if possible by air mail):

DESY **Bibliothek** **Notkestraße 85** **W-2000 Hamburg 52** **Germany**	**DESY-IfH** **Bibliothek** **Platanenallee 6** **O-1615 Zeuthen** **Germany**

DESY 93-047
April 1993

ISSN 0418-9833

Results from Pion Calibration Runs for the H1 Liquid Argon Calorimeter and Comparisons with Simulations

H1 Calorimeter Group

Abstract

We present results on calibration runs performed with pions at the CERN SPS for different modules of the H1 liquid argon calorimeter which consists of an electromagnetic section with lead absorbers and a hadronic section with steel absorbers. The data cover an energy range from 3.7 to 205 GeV. Detailed comparisons of the data and simulation with GHEISHA 8 in the frame work of GEANT 3.14 are presented. The measured pion induced shower profiles are well described by the simulation. The total signal of pions on an electromagnetic energy scale is reproduced to better than 3% in various module configurations. After application of weighting functions, determined from Monte Carlo data and needed to achieve compensation, the reconstructed measured energies agree with simulation to about 3%. The energies of hadronic showers are reconstructed with a resolution of about $50\%/\sqrt{E} \oplus 2\%$. This result is achieved by inclusion of signals from an iron streamer tube tail catcher behind the liquid argon stacks.

H1 Calorimeter Group

B. Andrieu[15], J. Bán[10], E. Barrelet[16], H. Bergstein[1], G. Bernardi[16], M. Besançon[20], E. Binder[8], H. Blume[13], K. Borras[6], V. Boudry[15], F. Brasse[8], W. Braunschweig[1], V. Brisson[14], A.J. Campbell[7], T. Carli[15], M. Colombo[6], Ch. Coutures[20], G. Cozzika[20], M. David[20], B. Delcourt[14], L. DelBuono[16], M. Devel[14], P. Dingus[15], A. Drescher[6], J. Duboc[16], O. Dünger[9], R. Ebbinghaus[6], S. Egli[22], N.N. Ellis[3], J. Feltesse[20], Y. Feng[16], F. Ferrarotto[19], W. Flauger[8,†], M. Flieser[13], K. Gamerdinger[13], J. Gayler[8], L. Godfrey[5], L. Goerlich[4], M. Goldberg[16], R. Grässler[2], T. Greenshaw[9], H. Greif[13], M. Haguenauer[15], L. Hajduk[4], O. Hamon[16], P. Hartz[6], V. Haustein[9], R. Haydar[14], W. Hildesheim[16], N. Huot[16], M.-A. Jabiol[20], A. Jacholkowska[14], M. Jaffre[14], H. Jung[2], F. Just[21], C. Kiesling[13], Th. Kirchhoff[8], F. Kole[5], V. Korbel[8], M. Korn[6], W. Krasny[4,20], J.P. Kubenka[13], H. Küster[8], J. Kurzhöfer[6], B. Kuznik[21], R. Lander[5], J.-F. Laporte[20], U. Lenhardt[6], P. Loch[8], D. Lüers[13,†], J. Marks[7], J. Martyniak[4], T. Merz[8], B. Naroska[9], A. Nau[8], H.K. Nguyen[16], F. Niebergall[9], H. Oberlack[13], U. Obrock[6], F. Ould-Saada[9], C. Pascaud[14], H.B. Pyo[8], K. Rauschnabel[6], P. Ribarics[13], M. Rietz[2], Ch. Royon[20], V. Rusinov[12], N. Sahlmann[2], E. Sánchez[13], P. Schacht[13], P. Schleper[1], W. von Schlippe[11], C. Schmidt[8], D. Schmidt[21], V. Shekelyan[12,6], H. Shooshtari[19], Y. Sirois[15], P. Staroba[17], M. Steenbock[9], H. Steiner[16], B. Stella[19], U. Straumann[22], J. Turnau[4], J. Tutas[1], L. Urban[13], C. Vallee[16], M. Vecko[17,15], P. Verrecchia[20], G .Villet[20], E. Vogel[1], A. Wagener[2], D. Wegener[6], A. Wegner[9], H.-P.Wellisch[13], T.P. Yiou[16], J. Žáček[14,18], Ch. Zeitnitz[8], F. Zomer[14]

[1] *I. Physikalisches Institut der RWTH, Aachen , Germany*[a]
[2] *III. Physikalisches Institut der RWTH, Aachen , Germany*[a]
[3] *School of Physics and Space Research, University of Birmingham, Birmingham, UK*[b]
[4] *Institute for Nuclear Physics, Cracow, Poland*
[5] *Physics Department and IIRPA, University of California, Davis, California, USA*[c]
[6] *Institut für Physik, Universität Dortmund, Dortmund, Germany*[a]
[7] *Department of Physics and Astronomy, University of Glasgow, Glasgow, UK*[b]
[8] *DESY, Hamburg, Germany*[a]
[9] *II. Institut für Experimentalphysik, Universität Hamburg, Hamburg, Germany*[a]
[10] *Institute of Experimental Physics, Slovak Academy of Sciences, Košice , Slovakia*
[11] *Queen Mary and Westfield College, London, UK*[b]
[12] *Institute for Theoretical and Experimental Physics, Moscow, Russia*
[13] *Max-Planck-Institut für Physik, München, Germany*[a]
[14] *LAL, Université Paris-Sud, IN2P3-CNRS, Orsay, France*
[15] *LPNHE, Ecole Polytechnique,IN2P3-CNRS, Palaiseau, France*
[16] *LPNHE, Universités Paris VI and VII, IN2P3-CNRS, Paris, France*
[17] *Institute of Physics, Czech Academy of Sciences, Praha, Czech Republic*
[18] *Nuclear Center, Charles University, Praha, Czech Republic*

[19] *INFN Roma and Dipartimento di Fisica, Universita "La Sapienzia", Roma, Italy*
[20] *DAPNIA, Centre d'Etudes de Saclay, Gif-sur-Yvette, France*
[21] *Fachbereich Physik, Bergische Universität Gesamthochschule Wuppertal, Wuppertal, Germany*[a]
[22] *Physik-Institut der Universität Zürich, Zürich, Switzerland*[d]
[†] *Deceased*

[a] *Supported by the Bundesministerium für Forschung und Technologie, FRG, under contract numbers 6AC17P, 6AC47P, 6DO57I, 6HH27I, 6MP17I, 6WT87P respectively*
[b] *Supported by the UK Science and Engineering Research Council*
[c] *Supported in part by USDOE grant DE F603 91ER40674*
[d] *Supported by the Swiss National Science Foundation*

1 Introduction

During the years 1989 and 1990 several calibration runs with different modules of the H1 liquid argon (LAr) calorimeter were performed at the H6 beam at the CERN SPS. The main goals of these runs were to provide an energy calibration for electrons [1] in the H1 detector [2], to study electron-hadron separation [3] and to determine energy calibration functions for hadrons and jets.

In previous papers [4,5] we reported on the performance of prototype LAr test modules. Here we present results achieved with final modules actually used in the H1 experiment at HERA. The emphasis is put on the comparison of pion signals from calibration measurements with corresponding simulations. This includes results for the fully reconstructed pion energy obtained with the H1 standard energy reconstruction code as used in the actual experiment, running on experimental and simulated signals from test beam events without any further change.

The H1 calorimeter is non-compensating (i.e. the signals from electrons are on average higher than those from pions of the same energy), but its high segmentation allows to distinguish electromagnetic (e.m.) and hadronic shower components and to reconstruct the hadronic energies by applying weighting functions (as discussed first in [6]) to the measured signals. The determination of such functions mainly from experimental data has already been studied by the H1 Calorimeter Group [4,5,7–9]. The quality of the Monte Carlo predictions for pion test data in the H1 calorimeters [10–14] now allows for extensive use of simulations for the determination of the parameters of these functions [11]. In this paper we first compare in various module configurations simulation and data for the mean total signal and other quantities characterizing the details of the shower development. We then study the deviations on the total hadronic energy reconstructed after having applied the same weighting functions to experimental and simulated data.

The outline of the paper is as follows: In sections 2 and 3 we briefly review the main features of the H1 LAr calorimeter and the experimental set-up in the test beam including the iron streamer tube tail catcher. The Monte Carlo simulation procedure is described in section 4. In section 5 we discuss the energy reconstruction first on the e.m. scale defined by electron calibration and then on the hadronic energy scale. Event selection criteria are given in section 6. Experimental data and simulation are compared in section 7 for several calorimeter modules in various test configurations. Results are presented for the total energy on the e.m. scale and after full reconstruction of weighted hadronic energy, the achieved energy resolutions, the effective electron-to-pion signal ratio, the longitudinal and lateral shower profiles and on signal distributions in single channels.

2 H1 Liquid Argon Calorimeter

The H1 LAr calorimeter at HERA covers an angular range of $4° \lesssim \theta \lesssim 154°$, where θ is measured with respect to the proton axis at HERA (fig. 1). The calorimeter consists of 8 wheels which are divided in azimuth into 8 modules (octants) in the barrel and into 2 modules in the forward region. The modules are divided into an inner, e.m. lead/LAr stack (EMC) and an outer, hadronic steel/LAr stack (HAC). The depth of the EMC varies between 30

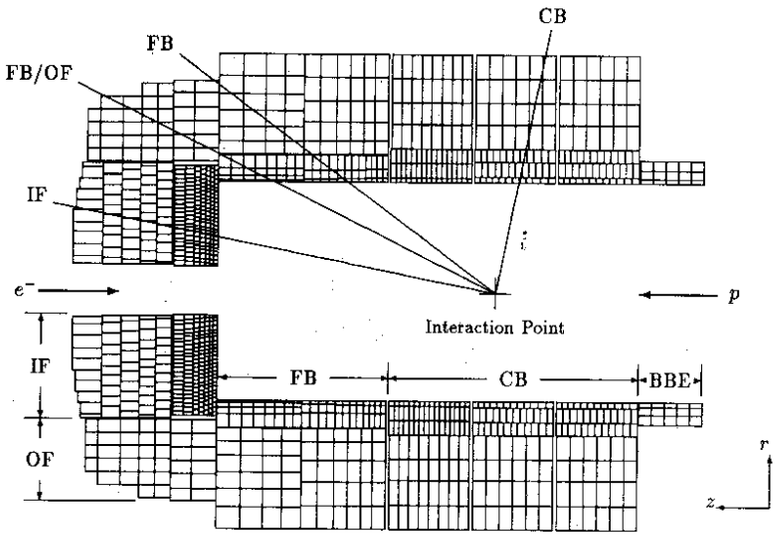

Figure 1: *Schematic view of the wheel and cell structure of the H1 liquid argon calorimeter. The lines from the interaction point indicate the directions of flight of the particles in the test beam set-up for the different calibration modules discussed here.*

radiation lengths (X_0) in the forward and 20 X_0 in the central barrel part corresponding to 1.4 and 1.0 interaction lengths (λ) for hadrons. The total depth for hadrons including the EMC is in the forward region of IF and FB/OF 6 and 8 λ respectively and near 5 λ in the barrel region (CB).

The calorimeter is highly segmented in both the e.m. and hadronic sections of the modules with a total of around 45000 geometric cells in a quasi projective geometry (fig. 1). The EMC has a 3 or 4 fold longitudinal segmentation while the HAC has 4 or 5 longitudinal segments. The lateral cell size in the forward region corresponds to about 1 Molière radius in the e.m. and 1 λ in the hadronic sections; the cells in the barrel region are typically twice this size.

The H1 LAr calorimeter is described in much more detail in [2,15].

3 Experimental Set-Up

The calibration program with electrons, pions and muons was performed in the H6 beam [16] at the CERN SPS. A survey of the set-up at the test beam is shown in fig. 2. The good homogeneity and stability of LAr calorimeters allows to calibrate single representative module configurations rather than each individual module of each calorimeter wheel.

3.1 Liquid Argon Calorimeter Configurations

In total 8 characteristic module configurations of the H1 LAr calorimeter (section 2) were tested in separate runs. In most cases the same modules were used as those later installed in the H1 cryostat at HERA. The configurations considered for this report are the inner forward calorimeter (IF, $\theta \approx 10°$), parts of the forward barrel and outer forward calorimeter (FB/OF, $\theta \approx 25°$), a section of the forward barrel alone (FB, $\theta \approx 34°$), and a part of the central barrel (CB, $\theta \approx 101°$) region. The modules were mounted into the cryostat such that the impact angle of the beam corresponds to the angle θ of a particle coming from the vertex of the ep collisions at HERA (fig. 1). The cryostat could house two complete H1 modules with the exception of IF, where an extra module of half the transverse size, but otherwise identical, was built for the purpose of calibration.

The same front end electronics scheme and calibration system as in H1 at HERA were used. The purity of the LAr was constantly monitored by probes identical to those in H1, positioned in the cryostat close to the calorimeter modules and consisting of a LAr ionisation chamber where the cathode coated with a ^{207}Bi source. More details can be found in [1,2,15].

3.2 Iron Streamer Tube Calorimeter

A warm iron-gascounter calorimeter (also called "tail catcher") with a depth of 4.5λ located behind the LAr modules allows for the measurement of hadronic shower tails and punch through pions. It consists of 10 iron plates (area 2.7 × 2.7 m^2, thickness 7.5 cm) interleaved with 10 streamer tube layers. In addition, three layers are mounted in front as well as behind the iron structure. The detector planes are equipped with read-out pads (typical size 30 × 30 cm^2) or strips. The digital read out of the wires (pitch 1 cm) and of the orthogonal strip electrodes (width 2 cm) serve for pattern recognition. The analog read out of the pad towers (two longitudinal segments of 5 pads/front-tower and 6 pads/back-tower, respectively) gives the energy measurement. The calorimeter has been calibrated in a stand-alone mode in the same beam line as the LAr calorimeter, using incident pions and muons. It is linear up to 40 GeV, the resolution amounts to $\sigma/E = 100\%/\sqrt{E\ (\mathrm{GeV})}$ (for details see [17,18]).

3.3 Beam

The set-up of the H6 beam line [16], the trigger elements and the beam counters are practically the same as in previous 1986-88 test runs [4]. The main beam defining elements are two Cerenkov counters used to select either electrons or pions and a set of multi-wire proportional chambers (MWPC's) to measure the horizontal and vertical beam positions. Typical measured values for the horizontal and vertical beam widths are $\sigma \approx 0.8$ cm for the lower beam energies around 5 – 10 GeV and $\sigma \approx 0.3$ cm for 80 GeV; the momentum spread is 0.5%. The systematic uncertainty of the beam energy scale is $15\%/p$ (GeV) $\oplus$ 0.5% [1]. The phase space of the particles is mainly defined by two narrow scintillation counters limiting the acceptance for the beam to an area of 3×3 cm^2. More detailed descriptions of the set-ups for the discussed run periods can be found in [1,11,13,18,19]

[1] N. Doble, private communication (1991).

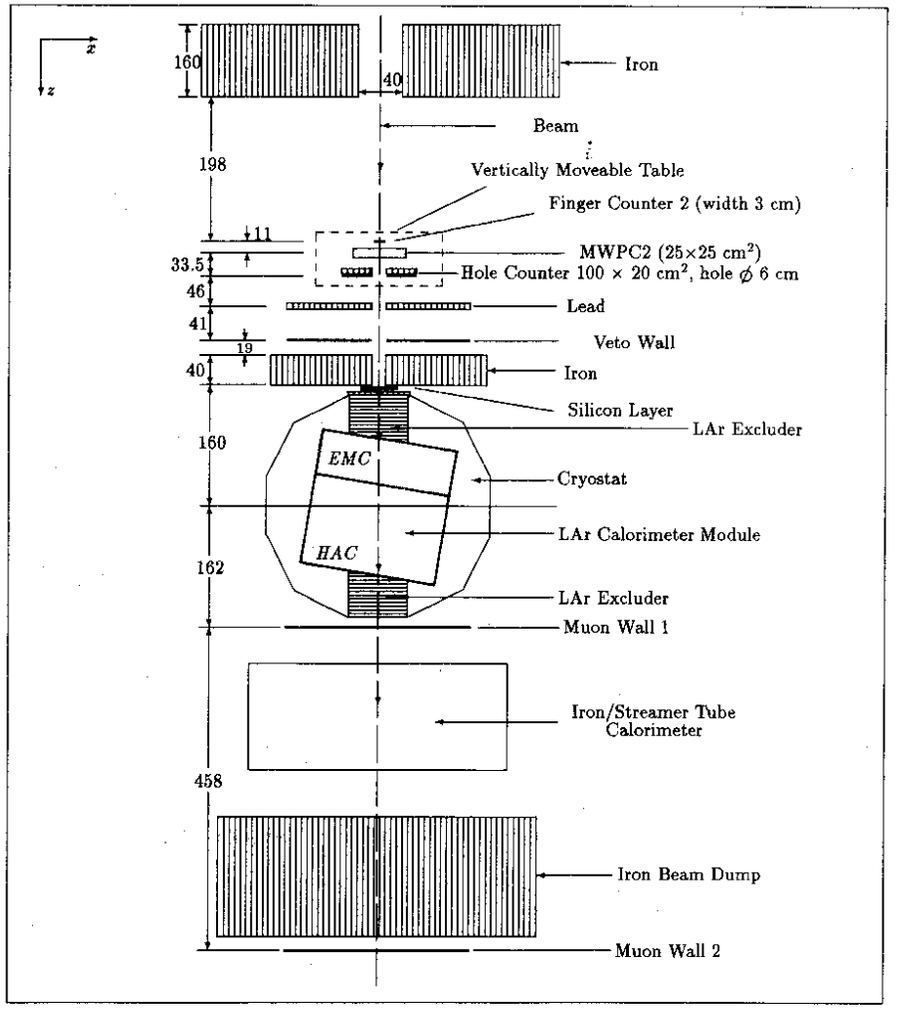

Figure 2: *Schematic view on the set-up in the test area at the H6 beam (dimensions in cm).*

4 Simulations

The calibration measurements have been simulated in the GEANT 3.14 [20] framework generating hadronic showers by GHEISHA 8 [21]. Electrons and photons produced in the hadronic showers are simulated with the default e.m. shower code of GEANT.

The simulation program contains a detailed description of the LAr calorimeter geometry and the gap and absorber structure which is identical to the standard H1 detector simulation. In addition it includes elements of the beam line, the cryostat and inactive material in front and behind the calibration modules. Also the central position of the beam, the spatial widths perpendicular to the beam axis and the known momentum spread (section 3.3) are simulated.

The thresholds for the tracking of particles in the simulation were set to 1 MeV for electrons/positrons, hadrons and to 0.2 MeV for photons.

Recombination effects were taken into account in the calculation of the signal. The energy dE deposited per simulation step dx in the liquid argon is corrected by Birks' Law [22]: $dE'/dx = dE/dx \cdot (1 + k_b dE/dx)^{-1}$, where dE' is the corrected deposited energy. A factor $k_b = 0.005$ g $\cdot$ MeV^{-1} $\cdot$ cm^{-2} was assumed (compare refs. [23]).

Each event is overlaid by an experimental empty event from a random trigger to include the effects of electronic noise (section 5.2).

For physics analyses H1 uses a faster simulation with parametrized e.m. showers [24] and hadron terminators [14]. The results for the simulation of pion beam data are practically identical to those of the detailed simulation discussed here [14,25].

5 Energy Reconstruction in the Liquid Argon Calorimeter

The energy reconstruction in the H1 LAr calorimeter involves several levels of charge corrections for experimental data [1,15] and channel selection and cluster finding algorithms for data and Monte Carlo. The charges and the energies deposited in the LAr for data and simulation respectively are first reconstructed cell by cell on an electromagnetic (e.m.) energy scale (see below). This procedure is independent of the particle type and is the same for test beam electrons or pions, or for jets at HERA. On this energy scale the experimental and simulated calorimeter response are directly comparable. In addition, all further energy corrections and applied weighting functions are exactly the same for measured and simulated signals.

In the following we will briefly describe the most important steps of the energy reconstruction for hadrons; further details follow in [2].

5.1 The Electromagnetic Energy Scale

The transformation of signals in the calorimeter to the e.m. energy scale is performed for experimental data by applying an electron calibration constant to the charge signal on the cell level. This constant has been determined for the EMC sections by calibration measurements with electrons [1]. Corrections for dead materials in front of the calorimeter or analysis cuts

calorimeter wheel name	EMC		HAC	
	c_{exp} [GeV/pC]	c_{sim}	c_{exp} [GeV/pC]	c_{sim}
CB	3.58	12.68	7.58	27.14
FB	3.41	12.76	6.70	25.23
IF	3.57	12.73	7.23	26.82
OF	–	–	6.70	24.93

Table 1: *The electron calibration constants used for experimental (c_{exp}) and for simulated (c_{sim}) signals for different wheels of the H1 LAr calorimeter. c_{sim} is just the inverse of the sampling fraction of electrons and therefore dimensionless.*

have been applied using detailed Monte Carlo simulation. For the hadronic sections, where no direct electron calibration measurements are yet available, the e.m. calibration constants are derived from the ones measured in the e.m. sections, correcting for the differences in the sampling fractions by detailed electron shower simulation using GEANT and EGS 4 [26] (compare [27]).

In case of simulation the energies deposited in the LAr layers are converted by multiplication with the effective inverse sampling fraction for simulated electrons.

The calibration constants used are given in table 1. The present uncertainty is $< 3\%$. The main error source is due to impurities in the LAr and the determination of the charge collection efficiency. For more details on the definition of the e.m. scale and the determination of the electron calibration constants see [1,28].

5.2 Noise Suppression

The typical electronic noise of a single channel is about $3.5 \cdot 10^4$ electrons, equivalent to 20 (40) MeV on the e.m. energy scale, in the EMC (HAC) sections. A channel selection based on the energy signal on this scale is performed to reduce the possible noise contributions to the total signal. The selection is identical for experimental and simulated events. To the latter realistic electronic noise was added by overlaying random trigger events. The following cuts are also applied in the general H1 reconstruction code [2]:

A certain channel i contributes to the signal of an event only if its absolute energy signal $|E_0^i|$ on the e.m. scale passes the condition:

$$|E_0^i| > 4 \cdot E_\sigma^i \quad \text{or} \quad \left(|E_0^i| > 2 \cdot E_\sigma^i \text{ and } E_0^j > 4 \cdot E_\sigma^j\right) \tag{1}$$

where E_σ^i, E_σ^j are the energy equivalents of the electronic noise of channels i, j, and j is a channel adjacent in space to channel i. Note that $E_\sigma > 0$ always, while the energy signal E_0^i might be positive or negative, in the latter case representing a pure noise contribution. Thus only weak thresholds are applied around a significant signal seed and statistical compensation of positive and negative noise contributions is achieved.

5.3 Hadronic Energy Reconstruction

Since in the H1 LAr calorimeter the response to hadrons is typically 30% smaller than that for electrons of the same incident energy, an additional correction has to be applied to the signal obtained on the e.m. scale.

The aim is to equalize the response to the e.m. and pure hadronic components of a hadronic shower and, therefore, to suppress the influence of the large fluctuations in the hadronic shower composition on the reconstructed energy. The technique exploits the fact that local energy deposits of high density are mainly of electromagnetic origin while the hadronic component is much more spread out. Thus, in a well segmented calorimeter the amount of energy deposited in the cells can be used for statistical separation of e.m. and hadronic energy depositions for which different correction factors are needed.

Signal weighting techniques to get the proper hadronic energy scale have already been studied for single pions in test beams [4–6]. The reconstruction of *ep* events at HERA, however, requires a good energy measurement also for jets in a wide energy range. Results of a first study of the application of weighting to signals from simulated jets have been presented in [7,8]. In the present approach the weighting functions are derived by simulation of jets in the full H1 detector thereby making use in the reconstruction of clustering of cells as described below. In the remaining part of this chapter the signals are assumed to be already reconstructed on the e.m. energy scale (section 5.1).

5.3.1 Clustering

All cells passing the noise suppressing step (section 5.2) are subject to clustering which is based on the correlation between signals in neighbouring cells. The aim is the formation of groups of cells with signals corresponding to particle showers. The algorithms used are tuned such that the cells containing energy depositions from an individual e.m. shower, initiated by a photon or electron in the jet, are most probably collected into one cluster. Hadronic clusters, on the other hand, with their large spatial fluctuations are in general split into several clusters [29].

Each cluster of cells with total energy above 1 GeV is classified to be either of e.m. or hadronic nature. The first are identified using characteristics like the fraction of cluster energy deposited in EMC (containment in EMC), in the first layer of EMC (early shower development), and in the four most energetic cells of a cluster (compactness), see ref. [3]. Clusters above 1 GeV which are not recognized as of e.m. type are called hadronic. At low energies clusters with significance $\sqrt{\sum (E_0^i/E_\sigma^i)^2} > 8$ and developing deeply inside the calorimeter are called hadronic as well.

5.3.2 Weighting Function Application

Electromagnetic clusters are regarded as being calibrated on the e.m. energy scale while signals in cells of hadronic objects have to be weighted. The latter are formed by cells which are not included into an e.m. cluster and located in a tube around a hadronic cluster ($r < 50$ cm in HAC and $r < 25$ cm in EMC).

The functions used to calculate the weights applied to signals in these cells are qualitatively the same as introduced in refs. [7,8], the weighted energy E_{rec}^i in a cell i is calculated

by:

$$E^i_{rec} = \left\{a_0 + a_1 \cdot \exp\left(-\alpha E^i_0 / V^i\right)\right\} \cdot E^i_0 \qquad (2)$$

where E^i_0 is the energy on the e.m. scale in this cell, V^i the volume of the cell, and a_0, a_1 and α are the parameters of the weighting function.

The parameters a_0, a_1 and α have to be determined for each calorimeter type (EMC, HAC). Two approaches to determine the weighting parameters as functions of quantities which are directly measurable inside the calorimeter alone have been studied. One possibility is to use simulated single pion response to determine the weighting parameters in different calorimeter wheels as functions of the signal of a hadronic cluster [11]. The other approach is to use the response to the hadrons in simulated jets to determine the parameters as functions of the reconstructed jet energy, calculated iteratively inside cones of 10 degree opening angle, as seen from the vertex. The results of the latter approach are applied in this paper. At low energies, below 7 GeV, the ansatz in eq. (2) is replaced by simple multiplicative factors corresponding to effective e/π ratios in EMC and HAC. In the region 7-10 GeV both methods contribute to the correction in order to get a smooth transition from the simple correction factors to the weighting according eq. (2).

We mention again, that there is no difference in the weighted energy reconstruction for jets and single hadrons or for simulated and experimental data, the same functions and parameters are used in all cases. The reconstructed energies for single pions shown in section 7 are obtained by running the above described standard H1 reconstruction algorithm – including the filtering of e.m. clusters – on the experimental and simulated signals.

6 Event Selection

Pions are selected by Cerenkov counters in the beam line (section 3). For beam energies $E_{beam} \geq 10$ GeV all events are accepted if their total signal E_0 on the e.m. energy scale fulfills $E_0 \gtrsim (2\text{–}4)$ GeV, depending on the depth of the actual module. This suppresses contributions from possible beam muons in case of experimental data; the cut is, however, applied to simulated data as well. No additional cut is applied against events with longitudinal energy leakage to avoid in the calibration at high incident energies a bias towards hadronic showers with a large electromagnetic content.

For those results where the iron streamer tube tail catcher is included, we veto against punch through by requiring to observe no digital hits in the last 3 layers of the tail catcher. They are located behind its last iron plate, i. e. behind 10.5 interaction lengths in total.

At lower energies, $E_{beam} \leq 7$ GeV, the muon contamination of the test beam can not be neglected either. Here the tail catcher and parts of the veto system behind the tail catcher are used to eliminate these muons. These selections lead of course to a suppression of such events in the data sample, where the pions are passing the LAr calorimeter with a late or no inelastic interaction.

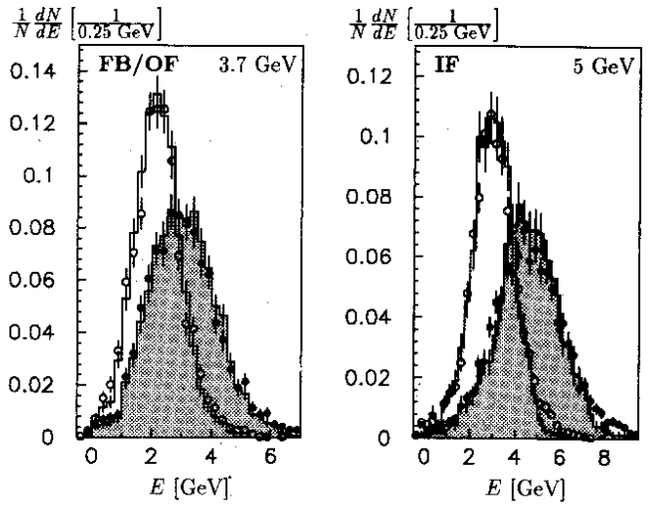

Figure 3: *Distributions of the energy on the electromagnetic scale E_0 (o simulations, histograms experiment) and of the reconstructed energy E_{rec} after weighting (• simulations, shaded histograms experiment) for the lowest available pion energies at the test beam.*

7 Experimental Results and Comparisons with Simulations

7.1 Total Energy Signals in Different Calorimeter Modules

Total energies are calculated by summing over the cells of the EMC and HAC sections of the LAr calorimeter, where each single channel has to pass the noise cut given in equation (1). Electronic noise is also included in case of simulation (section 5.2). Results on the e.m. scale (E_0) and hadronic energy scale (E_{rec}) are shown in fig. 3 for experimental and simulated pions at the lowest energies available in the IF and FB/OF calorimeter modules. The distributions agree quite well, besides somewhat larger tails towards high energies in case of simulation. Examples for pions at higher beam energies in various calorimeter regions are shown in fig. 4. The tails of the distributions to lower energies are due to pions with late or no inelastic interaction in the calorimeter. They are already at incident energies as low as 30 GeV more enhanced in the CB module which is shorter (total depth $d \approx 5\lambda$) than other modules such as FB ($d \approx 8\lambda$).

A comparison of the most probable reconstructed energies, based on fitted Gaussian distributions, for simulated and experimental pions as function of the beam energy is given in fig. 5. The maximal deviations are $< 3\%$ on the e.m. and $< 5\%$ on the hadronic energy scale. They are mainly systematic. A comparison of the results of the different stacks shows agreement better than $\pm 2\%$. If the results of the different stacks are averaged at a given

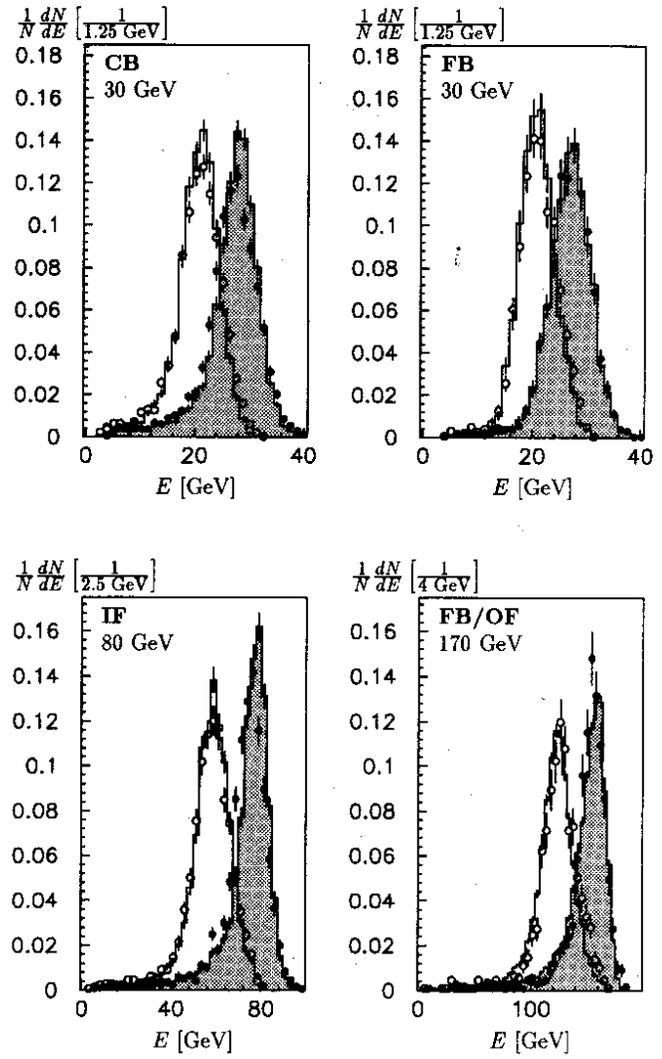

Figure 4: *Distributions of the energy on the electromagnetic scale E_0 (○ simulations, histograms experiment) and of the reconstructed energy E_{rec} after weighting (● simulations, shaded histograms experiment) at various incident energies in different calorimeter modules.*

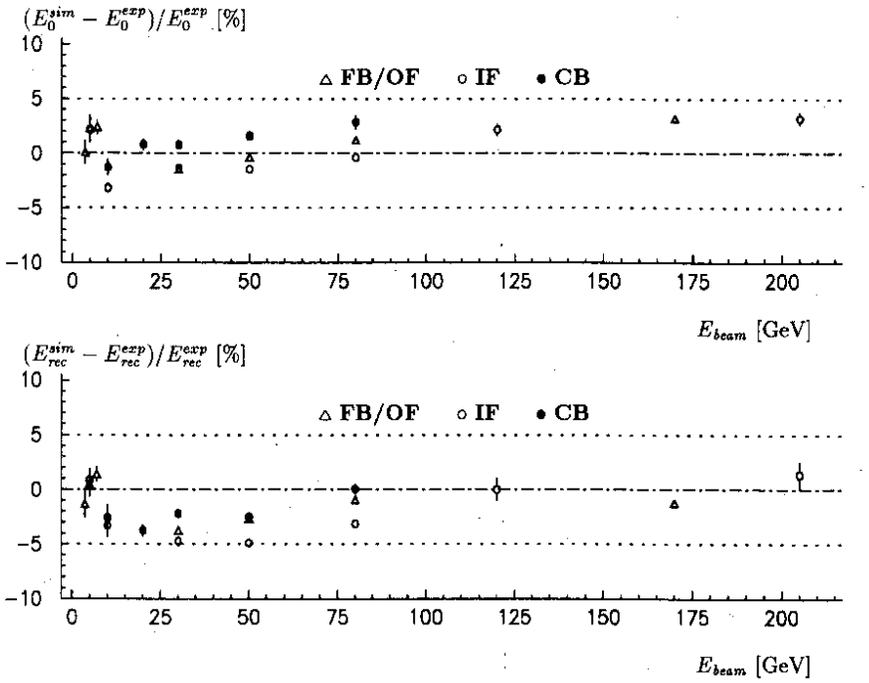

Figure 5: *The relative difference between simulated (E_0^{sim}) and experimental (E_0^{exp}) pion signals on the electromagnetic energy scale (top) and after weighting ($E_{rec}^{sim}, E_{rec}^{exp}$) (bottom), in three different calorimeter regions.*

beam energy, the deviations of simulation from experimental data are in the order of 3%. The reconstruction code applied to simulated events reproduces, under the condition of realistic electronic noise and analysis cuts, the energy deposited in the calorimeter to better than ±2%. Further studies of the calibration with the full detector at HERA are in progress [2].

The above results are based on the LAr calorimeter only. The inclusion of the tail catcher (section 3.2) is essential at high energies. This is visible in fig. 6 which shows the reconstruction at pion energies of 120 and 205 GeV with the LAr calorimeter alone (6λ) and together with the tail catcher (10.5λ in total).

7.2 Hadronic Energy Resolution

The energy resolution for pions is determined by fitting a Gaussian function to the distribution of fully reconstructed energies E_{rec}, as for example shown in figure 4, thereby excluding the low energy tails. The simulated distributions generally show larger fluctuations than the experimental data. This effect can be observed in all the different calorimeter modules.

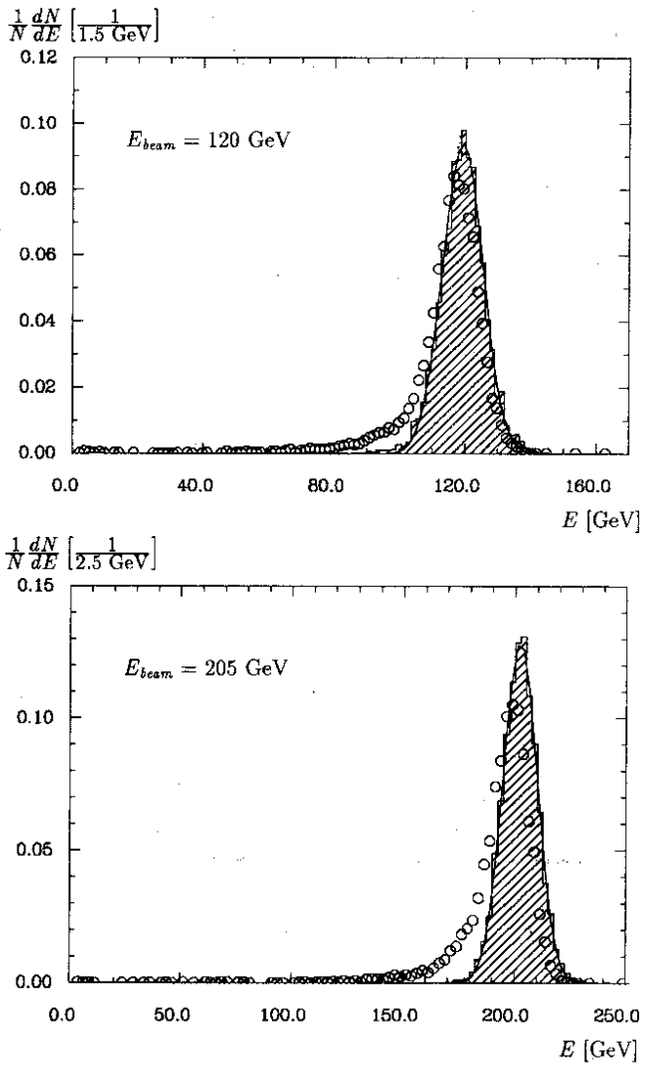

Figure 6: *Energy reconstruction for pions at 120 and 205 GeV for LAr module IF with tail catcher (hatched histogram) and IF only (○). Solid line: fitted Gaussian distribution.*

E_{beam}	electromagn. scale	
[GeV]	σ_{exp} [GeV]	σ_{sim} [GeV]
5	0.93±0.02	1.01±0.02
10	1.39±0.03	1.39±0.02
30	3.25±0.04	3.46±0.04
50	5.08±0.07	5.48±0.09
80	7.80±0.11	8.37±0.14
120	11.06±0.16	11.94±0.35
170	15.63±0.28	17.19±0.47
205	18.42±0.23	19.73±1.10

Table 2: *Variances of Gaussian distributions fitted to the total energy on the e.m. scale in the IF module for data and simulation with GHEISHA 8 (statistical errors).*

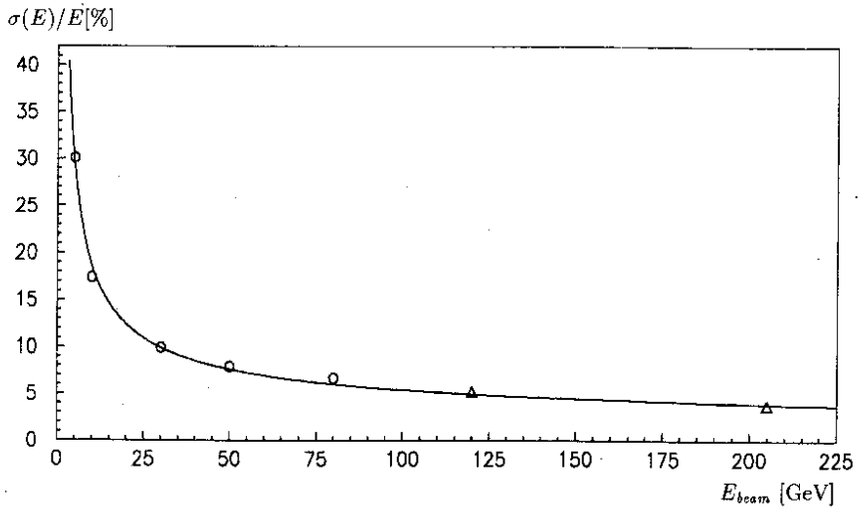

Figure 7: *Measured energy resolution for pions in the IF module (○) as function of the beam energy. The reconstruction at the higher energies includes signals from the tail catcher (△).*

Table 2 gives the direct comparison on the e.m. scale for the IF stack and shows that the resolution for simulation is on average worse by 7% than the measured one. These systematic effects are under study and some improvement of GHEISHA at high energies appears to be possible [30].

The measured energy resolution as a function of the beam energy is shown in fig. 7. The data are fully reconstructed on the hadronic energy scale (section 5.3). The signals from the tail catcher have been included at beam energies $E_{beam} > 80$ GeV to recover energies leaking out of the liquid argon calorimeter. The curve results from a fit to the data points, using the resolution function

$$\frac{\sigma(E)}{E} = \sqrt{\frac{a^2}{E_{beam}} + \frac{b^2}{E_{beam}^2} + c^2} \qquad (3)$$

with a stochastic term $a/\sqrt{E_{beam}}$, a noise term b/E_{beam} and a constant term c. This fit yields

$$a = (50.7 \pm 0.7)\% \cdot \sqrt{\text{GeV}}, \quad b = (945 \pm 32)\ \text{MeV}, \quad c = (1.6 \pm 0.1)\%.$$

which can be regarded as typical values for the whole calorimeter. As $c \sim (e/\pi - 1)$ [31], the relatively small constant term in equation (3) shows the good compensation achieved with the weighting functions.

7.3 Effective Electron-to-Pion Signal Ratio in the Liquid Argon Calorimeter

The energy E_0 reconstructed on the e.m. scale is a very good estimate of the energy E_{dep} deposited in the calorimeter in case of electrons, however it is on average smaller than E_{dep} or E_{beam} in case of incident pions.

The electron-to-pion signal ratio on the e.m. scale can be expressed by:

$$\frac{e}{\pi} = \frac{\langle E_{dep} \rangle}{\langle E_0 \rangle} \qquad (4)$$

As E_{dep} is known exactly only for Monte Carlo events, we have calculated an effective $(e/\pi)_{eff}$ for different calorimeter wheels and pion energies E_{beam}:

$$\left(\frac{e}{\pi}\right)_{eff} = \frac{E_{beam}}{\langle E_0 \rangle} \qquad (5)$$

This quantity overestimates the e/π ratio, since it is affected by energy losses due to material in front of the calorimeters, limited lateral acceptance of the calibration modules and, especially at high beam energies, by longitudinal energy leakage. Measured values of $(e/\pi)_{eff}$ are shown in fig. 8a. Simulations yield similar results for $(e/\pi)_{eff}$ on the level of agreement observed in fig. 5. The shorter CB module shows a different dependence on E_{beam} than the deeper IF and FB/OF. This is due to longitudinal energy leakage, which occurs in case of the CB module already significantly at beam energies around 30 GeV, leading even to a soft rise of $(e/\pi)_{eff}$ with increasing E_{beam}. The two deeper modules, IF and FB/OF, show practically the same absorption characteristics in terms of the energy dependence of $(e/\pi)_{eff}$.

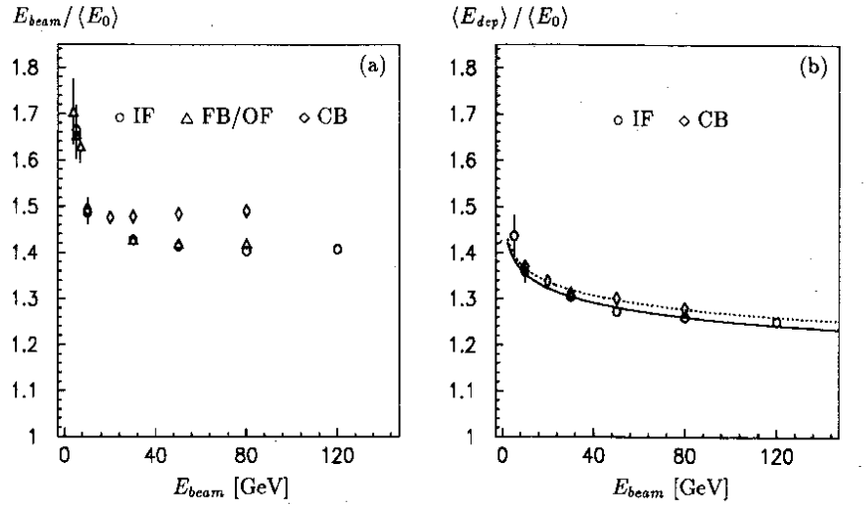

Figure 8: *The effective electron-to-pion signal ratio calculated as given in equation (5) for experimental pions, as function of the beam energy E_{beam} in different calorimeter regions (a). Picture (b) shows e/π corrected by Monte Carlo for the effect of limited acceptance and longitudinal energy leakage. The curves show results from fits, as discussed in the text.*

The quantity e/π, as given in equation (4), has also been calculated correcting for leakage by simulation, for which the deposited energy is known event by event (fig. 8b). The resulting e/π is falling with increasing particle energy, as expected, and is very similar for all the studied modules. The curves in fig. 8b are fits with functions falling linearly with increasing $\log E_{beam}$. This behaviour corresponds to a rise of the intrinsic electromagnetic fraction $f_{em} \sim \log E_{beam}$ of the hadronic shower [5,32].

7.4 Shower profiles

Longitudinal and transverse shower profiles have been measured at different beam energies and are compared with Monte Carlo simulation. The IF and CB calorimeter modules are especially well suited for this study because of the approximately perpendicular impact direction of the beam particles into these stacks.

Figure 9 shows the average relative energy deposit, measured on the e.m. energy scale and normalized to the depth of each longitudinal segment, as a function of the calorimeter depth for pions at different beam energies in the IF and CB modules. In general the simulation follows quite well the experimental data. Some discrepancies are visible in the first segments of the hadronic stacks.

The transverse profiles for experimental and simulated pions at 5, 30 and 80 GeV in the IF module are compared in fig. 10. The average relative energy loss, integrated over the whole shower depth, is shown as function of the perpendicular distance from the shower axis,

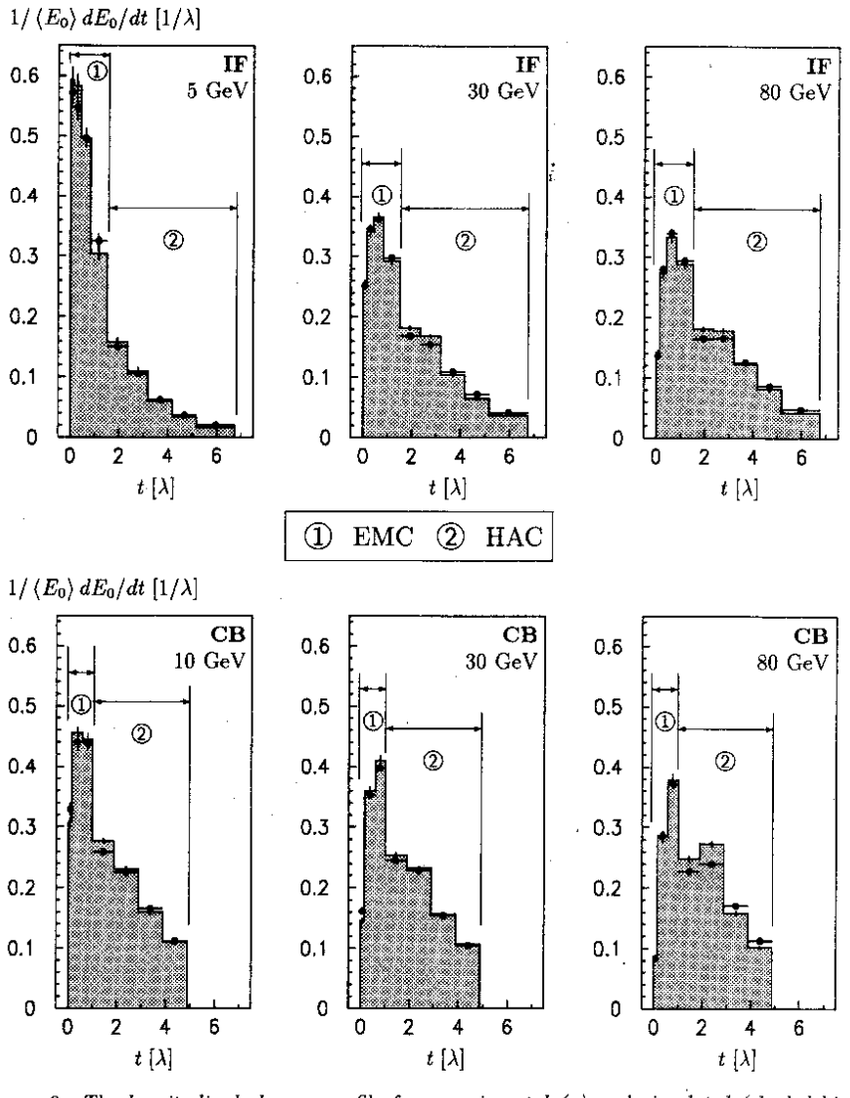

Figure 9: *The longitudinal shower profile for experimental (•) and simulated (shaded histograms) pions at three different beam energies in IF and CB. Shown is the average relative energy deposition $dE_0/\langle E_0\rangle$, as measured on the e.m. scale per unit absorption length λ, as a function of the calorimeter depth t.*

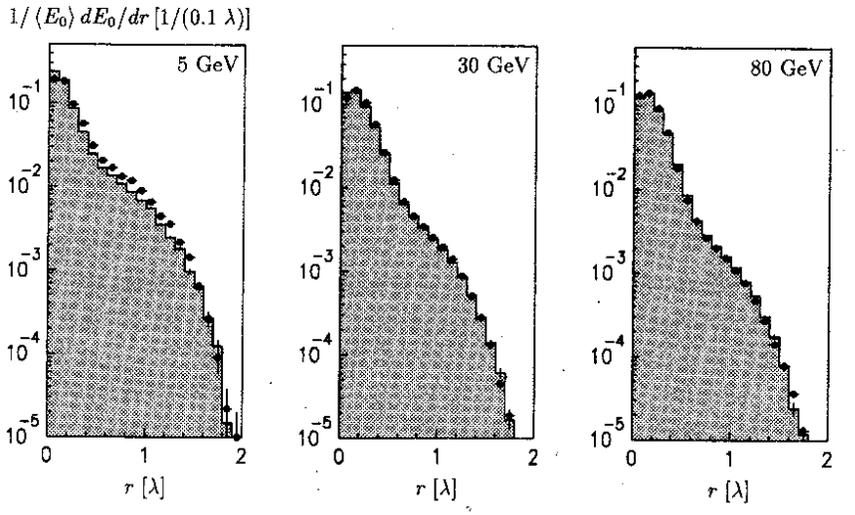

Figure 10: *The transverse shower profiles for pions at different energies in the IF module, experiment (•) and simulation (shaded histograms). The average relative energy deposition $dE_0/\langle E_0\rangle$, measured on the e.m. scale and integrated over the whole shower depth, is shown as function of the distance r from the shower axis.*

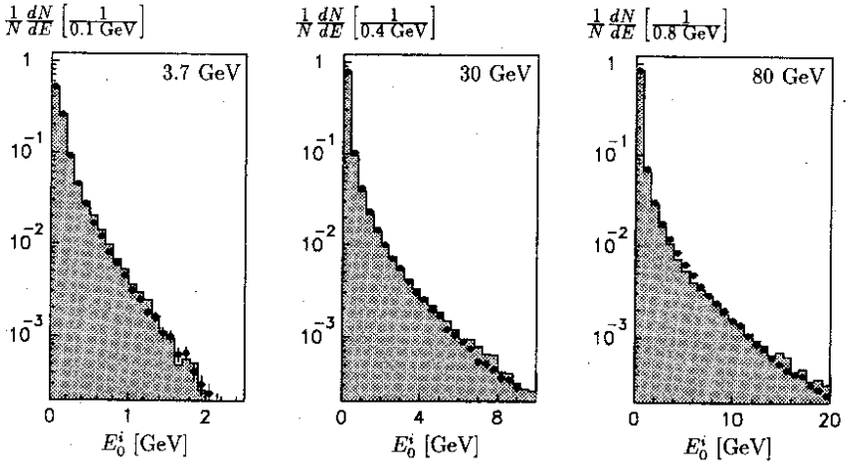

Figure 11: *The distributions of signals E_0^i in single cells for experimental (•) and simulated (shaded histograms) pions in the FB/OF region, at different beam energies.*

which is measured for each event by determining the impact point at the front face of the calorimeter and the center of gravity of the shower. The lateral acceptance of the module is limited to about 2 λ.

7.5 Signals in Single Channels

In fig. 11 we compare fluctuations of energies E_0^i of individual cells averaged over the FB/OF calorimeter modules at pion beam energies of 3.7, 30 and 80 GeV. The simulation follows very well the distribution of the energies E_0^i over several orders of magnitude in probability. This is important if, as in the present energy reconstruction scheme for the H1 LAr calorimeter, the determination of weighting functions is based on simulation of hadrons or jets. The weights applied in the hadronic energy reconstruction (section 5.3) to the signal energies E_0^i are functions of these energies themselves.

8 Conclusions

Detailed comparisons of signals from pions in H1 liquid argon calorimeter modules and simulation in the GEANT/GHEISHA frame have been presented on the electromagnetic energy scale which is determined from electron measurements. The total signal for pions is described within an uncertainty of $< 3\%$ for beam energies between 3.7 and 205 GeV. The longitudinal and lateral shower spreads are well reproduced by the simulation. The same is true for energy fluctuations in single cells.

Full reconstruction of the energy deposited by single pions in the calorimeter can be achieved by signal weighting functions determined from simulated jets. Here the deviations of experimental and simulated energies are about 3%. An energy resolution of about $50\%/\sqrt{E\ (\mathrm{GeV})}$ with a constant term below 2% is achieved.

Acknowledgements

We appreciate the big efforts of all the technical collaborators who constructed and maintained the calorimeters. The support of the CERN staff operating the SPS, the H6 beam line and the computer facilities is gratefully acknowledged. We thank all funding agencies for financial support. Finally we would like to thank H. Fesefeldt for useful discussions.

References

[1] H1 Calorimeter Group, *Calibration of the H1 Liquid Argon Calorimeters by Electrons*, in preparation.

[2] H1 Collab., *The H1-Detector at the Electron-Proton Storage Ring HERA*, to be submitted to Nucl. Instr. and Meth.

[3] H1 Calorimeter Group, B. Andrieu et al., *Electron Identification in Liquid Argon Calorimeters*, Proceedings of the 3rd Int. Conf. on Advanced Technology and Particle Physics, Como, Italy (June 1992), to be published in Nucl. Phys. B (Proc. Suppl.).

[4] H1 Calorimeter Group, W. Braunschweig et al., Nucl. Instr. and Meth. A265 (1988) 419; ibid, A275 (1989) 246.

[5] H1 Calorimeter Group, W. Braunschweig et al., *Results from a Pb-Fe Liquid Argon Calorimeter*, DESY internal report, DESY 89-022 (1989).

[6] J. P. Dishaw et al., Phys. Lett. B85 (1979) 142; J. P. Dishaw Slac-Report-216 (1979); CDHS Collab., H. Abramowicz et al., Nucl. Instr. and Meth. 180 (1981) 429.

[7] H1 Calorimeter Group, H. Jung et al., *Study of Software Compensation for Single Particles and Jets in the H1 Calorimeter*, contributed paper to the XXV Int. Conf. on High Energy Physics, Singapore (1990).

[8] H. Greif *Untersuchungen zur kalorimetrischen Messung von Jeteigenschaften in hochenergetischen Elektron-Proton Speicherring-Experimenten*, MPI-PAE/Exp.El. 229 (1990), Thesis, Technical University of München, 1990.

[9] J. Marks, *Eigenschaften eines Kalorimeters aus Blei und Kupfer in flüssigem Argon zur Messung hochenergetischer Jets unter besonderer Berücksichtigung einer Reduktion der Schauerfluktuationen*, DESY F21-90-01 (1990), Thesis, University of Hamburg, 1989.

[10] J. Gayler, *Simulation of H1 Calorimeter Test Data with GHEISHA and FLUKA*, in MC91, Workshop of Detector and Event Simulation, ed. K. Bos and B van Eijk, NIKHEF-H, Amsterdam (1991), p 312.

[11] P. Loch, *Kalibration des H1 Flüssig-Argon Kalorimeters unter Berücksichtigung der Gewichtungsmethode für Teilchenjets*, DESY FH1K-92-02, Thesis, University of Hamburg, 1992.

[12] J. Žáček et al., *Comparison of Pion Calorimeter Test Data with Simulation for CB2/CB3 Period*, H1 Internal report, H1-04/92-220 (1992);
E. Sánchez, *Comparison of the Calorimeter Calibration Data with Simulation for the FB1/FB2 Period*, ibid, H1-07/92-232 (1992).

[13] M. Flieser, *Untersuchungen zur Energieauflösung eines Flüssig-Argon-Kalorimeters für Elektronen und Pionen im Energiebereich von 3.7 - 170 GeV*,
MPI-Phe/92-08, Diploma Thesis, Technical University of München, 1992.

[14] M. Rudowicz, *Hadronische Schauersimulation für den H1 Detektor*,
MPI-PhE/92-14, Thesis, University of Hamburg, 1992.

[15] H1 Calorimeter Group, B. Andrieu et al., *The H1 Liquid Argon Calorimeter System*, to be submitted to Nucl. Instr. and Meth.

[16] *H6 Beam Tuning*, CERN preprint, SPS/EPB/PC (1981).

[17] H1 Muon Group, H. Bergstein et al., *Beam calibration of the H1 tail catcher at Cern*, H1 internal report, H1-10/91-197 (1991) and *The tail catcher test stack at CERN in 1992; detector setup and software analysis tools*, ibid, H1-01/93-261 (1993).

[18] H. Bergstein, *Gesamteichung des H1 Eisenjochkalorimeters*, Thesis, RWTH Aachen, 1993.

[19] J.-F. Laporte, *...Calibration Absolue de la Mesure en Energie d'un Electron dans le Calorimètre à Argon Liquide de l'Expérience H1*, Thesis, University of Paris-Sud, 1991;
R. Haydar, *Test et Calibration du Calorimètre Hadronique de l'Expèrience H1 à HERA*, Thesis, University of Paris-Sud, 1991;
R. Grässler, *Kalibration eines elektromagnetischen Kalorimetermoduls für den H1-Detektor*, Diploma Thesis, RWTH Aachen, 1991.

[20] R. Brun et al., *GEANT 3 Manual*, CERN DD/EE/84-1 (1987).

[21] H. Fesefeldt, *The Simulation of Hadronic Showers – Physics Applications –* , PITHA-Report 85-02, RWTH Aachen (1985).

[22] J.B. Birks, Proc. Phys. Soc. **64** (1951) 874.

[23] C.W. Fabjan et al., Nucl. Instr. and Meth. 141 (1977) 61;
J. Brau and T. A. Gabriel, ibid, A238 (1985) 489.

[24] S. Peters, *Die parametrisierte Simulation elektromagnetischer Schauer*, MPI-PhE/92-13, Thesis, University of Hamburg, 1992.

[25] M. Kuhlen, *The Fast H1 Detector Monte Carlo*, to be published in the proceedings of the 26th Int. Conf. on High Energy Physics, Dallas ,1992.

[26] R.L. Ford and W.R. Nelson, *The EGS code system*, SLAC-Report-210 (June 1978); SLAC preprint, EUN-SLAC-0 (May 1983).

[27] R. Tamoschat, *Untersuchungen zum Photon- und Elektronnachweis mit dem H1-Detektor unter Berücksichtigung des Magnetfeldes*, Diploma Thesis, University of Dortmund, 1992.

[28] J. Gayler, H. Küster and P. Loch, *Determination of the Electromagnetic Scale for the IF Calorimeter*, H1 Internal report, H1-04/91-171 (1991) .

[29] L. Görlich and H.P. Wellisch, *Documentation of the LAr Clustering*, H1 Internal report, H1-12/91-204 (1991).

[30] A. Wagener, *Optimierung von Simulationsrechnungen hadronischer Schauer in einem Flüssig-Argon-Kalorimeter*, PITHA-Report 92/37, Diploma Thesis, RWTH Aachen (1992).

[31] R. Wigmans, Nucl. Instr. and Meth. A259 (1987) 389.

[32] C.W. Fabjan, *Calorimetry in High Energy Physics*, CERN preprint, EP/85-54 (1985).